Globally Defined Dynamic Modelling and Geometric Tracking Controller Design for Aerial Manipulator

Byeongjun Kim, Dongjae Lee, Jeonghyun Byun and H. Jin Kim

***Abstract*— This study presents a globally defined dynamics for a conventional multirotor equipped with a single n-DOF manipulator using modified Lagrangian dynamics. This enables the reformulation of entire dynamics directly on $\mathsf{SO}(3)$ without exploiting any local coordinates, and thus problems such as the singularity of Euler angles can be avoided. Since skew-symmetric property of Coriolis matrix C and inertia matrix facilitates stability analysis, we propose a method to compute C which guarantees the skew-symmetric property by considering C as a summation of two sub matrices. Then, a geometric tracking controller is designed based on decoupled dynamics applying passive decomposition. The proposed controller guarantees almost global region of attraction. We validate our method via consecutive aerial flipping experiments.**

I. INTRODUCTION

Aerial manipulator has accomplished challenging tasks by attaching multi-DOF manipulator to multirotor such as pick and place [1], bridge inspection [2], interaction with movable structure [3] and plug-pulling [4]. However, most research on aerial manipulators, including the above studies, use Euler angle to describe and control the attitude of systems. This implies that the superior maneuverability of the aerial platform is not fully exploited and thus the robot may fail to carry out given missions due to the singularity problem. Furthermore, singularity of Euler angle limits theoretical developments for controller design and stability analysis. For instance, they may not guarantee successful accomplishment of given missions if attitude is suddenly disturbed. Another problem is that, since most aerial manipulators have a single manipulator attached to top or bottom of the platform, performing tasks on the other side of attached surface is impossible due to attitude limitation. One may try attaching an extra or a very long manipulator to enlarge the workspace of platform, but this is extremely inefficient because the multirotor base is vulnerable to inertia.

These problems are resolved if aerial manipulator is capable of aerial flipping or recovering from huge attitude error even over 90°. To do so, in this work, we describe attitude of the platform without employing Euler angle representation and design a geometric tracking controller which guarantees a large region of attraction.

A. Related works

Complicated equations of motion for a single general aerial manipulator platform were derived using the standard Euler-Legrange equation [5] popular for its effectiveness in deriving the dynamics of a multibody system. However, to use the standard Euler-Lagrange equation of motion, singularity is unavoidable because the attitude of the system must be described as three scalar variables, i.e., Euler angles.

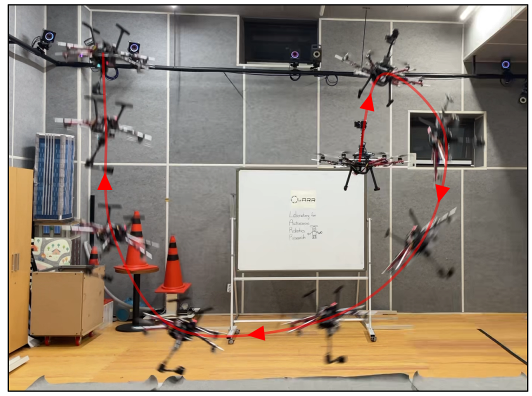

Fig. 1. A sequential image of aerial manipulator changing flight mode from normal flight to inverted flight through aerial flipping. Arrow direction describes motion of the platform.

For bare multirotors that have simpler dynamics of a single rigid body, geometric tracking controllers have been extensively developed [6-9]. Still, they cannot be directly employed for aerial manipulators. Since [6] and [7] only consider multirotor itself, dynamic effects of manipulators will harm the stability. The robust geometric controllers in [8] and [9] can only guarantee the uniform boundedness of stability at best, even when the model parameters of attached manipulator are exactly known. In addition, their assumptions of bounded disturbances limits the applicability of manipulators.

B. Contributions

Main contributions of this study are summarized as follows:

- To the best of our knowledge, this is the first attempt to explicitly reveal globally defined dynamics of an aerial manipulator using rotation matrices and angular velocities instead of local description of $\mathsf{SO}(3)$. The modified Lagrangian dynamics [10] allows direct derivation of the attitude dynamics on $\mathsf{SO}(3)$ so that problems of local coordinates such as singularities can be avoided.
- We propose Coriolis matrix which assures the skew-symmetric property facilitating stability analysis although a direct use of the Christoffel symbol is restricted because of difference between the modified Euler-Lagrange equation and the standard one.
- A geometric controller is presented based on decoupled dynamics applying passive decomposition. We can guarantee the almost global exponential stability for

attitude and joint angle dynamics and almost global exponential attractiveness for complete dynamics. A real-world experiment of consecutive aerial flipping demonstrates the above mentioned stability.

C. Notations

Throughout this paper, quantities with subscripts b and i refer to the quantities of the multirotor base and the i-th link, respectively. The j-th element of a vector $*$ is denoted by $*_j$. For a matrix A, the i-th row and the j-th column element is represented as a_{ij} with the corresponding lower-case letter. $\lambda_M(*)$ and $\lambda_m(*)$ stand for the largest and smallest eigenvalue of square matrix $*$, respectively. $\texttt{blkdiag}\{A, B\}$ refers to a block diagonal matrix which consists of matrices A and B. $\|*\|$ indicates a 2-norm of a vector or induced 2-norm of a matrix. The *hat map* $(\cdot)^\wedge : \mathbb{R}^3 \to \mathfrak{so}(3)$ is defined as the skew-symmetric matrix representation of the vector cross product. The *vee map* $^\vee : \mathfrak{so}(3) \to \mathbb{R}^3$ is the inverse of the hat map. $I_{n\times n}$ and $0_{n\times m}$ denote $n \times n$ identity matrix and $n \times m$ zero matrix, respectively.

II. DYNAMICS REFORMULATION

In this section, dynamics of a conventional multirotor equipped with a n-DOF robotic manipulator is reformulated using the modified Lagrangian dynamics [10] which enables direct formulation of the attitude dynamics on $\mathsf{SO}(3)$ without exploiting Euler angle representation.

A. Kinematics

Let us define the reference frame and the body frame as O_I and O_B, respectively, using North-West-Up convention. The center of mass position of the multirotor base expressed in O_I, rotation matrix from O_B to O_I, and joint angles are represented as $p \in \mathbb{R}^3, R \in \mathsf{SO}(3)$ and $\theta \in \mathbb{R}^n$, respectively. $p_i^B \in \mathbb{R}^3$ denotes the center of mass position of the i-th link expressed in O_B. Let $p_i^I \in \mathbb{R}^3$ indicate the center of mass position of the i-th link expressed in O_I, $\omega \in \mathbb{R}^3$ refer to body angular velocity expressed in O_B, $\omega_i^i \in \mathbb{R}^3$ represent angular velocity of the i-th link expressed in the i-th link frame. $J_{i,t} \in \mathbb{R}^{3\times n}$ and $J_{i,r} \in \mathbb{R}^{3\times n}$ are Jacobian matrices. $R_i^B \in \mathsf{SO}(3)$ is the rotation matrix from the i-th link frame to O_B. Defining the generalized velocity as $\dot{q} = [\dot{p}^\top \ \omega^\top \ \dot{\theta}^\top]^\top$, the following matrix form simplifies the kinematic relations.

$$\dot{p} = [I_{3\times3} \ \ 0_{3\times3} \ \ 0_{3\times n}]\dot{q} = M_{b,t}\dot{q} \tag{1}$$

$$\omega = [0_{3\times3} \ \ I_{3\times3} \ \ 0_{3\times n}]\dot{q} = M_{b,r}\dot{q} \tag{2}$$

$$\dot{p}_i^I = [I_{3\times3} \ \ -Rp_i^{B\wedge} \ \ RJ_{i,t}]\dot{q} = M_{i,t}\dot{q} \tag{3}$$

$$\omega_i^i = {R_i^B}^\top [0_{3\times3} \ \ I_{3\times3} \ \ J_{i,r}]\dot{q} = M_{i,r}\dot{q} \tag{4}$$

B. Modified Euler-Lagrangian Approach

Configuration of the entire system can be uniquely determined by p, R and θ Let the Lagrangian of the system be $\mathcal{L} = \mathcal{T} - \mathcal{U}$ where $\mathcal{T}$ and $\mathcal{U}$ refer to the sum of the total kinetic and potential energy of the system, respectively. Then, defining action integral and considering infinitesimal variations, one

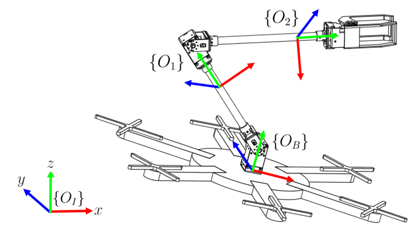

Fig. 2. Overall platform and frame description

can reach the following Modified Euler-Lagrange equations of motion. Detailed derivation for attitude dynamics can be found in [10].

$$\frac{d}{dt}\left(\frac{\partial \mathcal{L}}{\partial \dot{p}}\right) - \frac{\partial \mathcal{L}}{\partial p} = \tau_p \tag{5}$$

$$\frac{d}{dt}\left(\frac{\partial \mathcal{L}}{\partial \omega}\right) + \omega^\wedge \frac{\partial \mathcal{L}}{\partial \omega} + \textstyle\sum_{l=1}^{3} r_l{}^\wedge \frac{\partial \mathcal{L}}{\partial r_l} = \tau_R \tag{6}$$

$$\frac{d}{dt}\left(\frac{\partial \mathcal{L}}{\partial \dot{\theta}}\right) - \frac{\partial \mathcal{L}}{\partial \theta} = \tau_\theta \tag{7}$$

where τ_p, τ_R and τ_θ indicate generalized forces, and $r_l^\top$ is the l-th row of R.

The total kinetic energy is considered as $\mathcal{T} = \frac{1}{2}\dot{q}^\top M \dot{q}$ using the inertia matrix $M \in \mathbb{R}^{6+n\times 6+n}$ computed as the following equation

$$M(R, \theta) = M_{b,t}^\top m_b M_{b,t} + M_{b,r}^\top I_b M_{b,r} + \textstyle\sum_{i=1}^{n} M_{i,t}^\top m_i M_{i,t} + M_{i,r}^\top I_i M_{i,r} \tag{8}$$

where m and I indicate the mass and moment of inertia matrix, respectively. The potential energy $\mathcal{U}$ of the system is

$$\mathcal{U} = m_b g e_3^\top p + \textstyle\sum_{i=1}^{n} m_i g e_3^\top (p + Rp_i^B).$$

By substituting $\mathcal{T}$ and $\mathcal{U}$ calculated above into (5)-(7), one can obtain the following standard matrix form of equations of motion

$$M\ddot{q} + C\dot{q} + G = \tau \tag{9}$$

where $C \in \mathbb{R}^{6+n\times 6+n}, G \in \mathbb{R}^{6+n}$ and $\tau \in \mathbb{R}^{6+n}$ indicate the Coriolis-centrifugal matrix, gravity vector and generalized force vector, respectively. For the conventional multirotor platform, a control input can be chosen as $u = [T \ \ u_b^\top \ \ u_\theta^\top]^\top$ where $T \in \mathbb{R}^1, u_b \in \mathbb{R}^3$, and $u_\theta \in \mathbb{R}^n$ are net thrust along body z-axis, body torque expressed in O_B, and joint torques, respectively. Consequently, deploying the virtual work principle, generalized force τ in (9) is determined as $\tau = [(TRe_3)^\top \ u_b^\top \ u_\theta^\top]^\top$.

C. Skew-symmetricity of $\dot{M} - 2C$

For the term $C\dot{q}$ from (9), it is well-known that the matrix representation of C is not unique. Furthermore, existing studies on designing controllers and proving stability for multi-body mechanical systems have widely harnessed the above skew-symmetricity [5], [11], [12]. This implies that, to apply the similar controller design procedure used in previous studies for the proposed dynamics, the skew-symmetricity of $\dot{M} - 2C$ should be verified. However, unlike [5], it is impossible to directly utilize the Christoffel symbols to calculate C such that the skew-symmetricity of

$\dot{M}-2C$ holds, since (6) is dissimilar from the standard Euler-Lagrange equation. Thus, this subsection provides a method to compute C which guarantees the skew-symmetricity of $\dot{M}-2C$.

First, the total kinetic energy can be rewritten as

$$\mathcal{T} = \tfrac{1}{2}\textstyle\sum_{i=1}^{6+n}\sum_{j=1}^{6+n} m_{ij}\dot{q}_i\dot{q}_j. \tag{10}$$

Since the potential energy does not depend on $\dot{q}$, the time derivative terms of (5)-(7) become

$$\frac{d}{dt}\left(\frac{\partial\mathcal{L}}{\partial\dot{q}_k}\right) = \frac{d}{dt}\sum_{j=1}^{6+n} m_{kj}\dot{q}_j = \sum_{j=1}^{6+n}\left(m_{kj}\ddot{q}_j + \frac{dm_{kj}}{dt}\dot{q}_j\right).$$

The inertia matrix M is also irrelevant with $\dot{q}$. Accordingly, the last term of the above equation can be replaced with

$$\sum_{j=1}^{6+n}\tfrac{dm_{kj}}{dt}\dot{q}_j = \sum_{i=1}^{6+n}\sum_{j=1}^{6+n}\tfrac{1}{2}\left(\tfrac{\partial m_{kj}}{\partial q_i} + \tfrac{\partial m_{ki}}{\partial q_j}\right)\dot{q}_i\dot{q}_j$$

where the following terms are additionally defined using $\dot{R} = R\omega^\wedge$ for the case of $i,\ j = 4,\ 5,\ 6$.

$$\begin{bmatrix}\frac{\partial m_{kj}}{\partial q_4} & \frac{\partial m_{kj}}{\partial q_5} & \frac{\partial m_{kj}}{\partial q_6}\end{bmatrix}^\top := -\sum_{l=1}^{3} r_l{}^\wedge\frac{\partial m_{kj}}{\partial r_l} \tag{11}$$

Here, note that, the derivative form is adopted only for the notational consistency.

For further development, let us separately consider two cases: 1) $k = 4,5,6$ and 2) $k \neq 4,5,6$. The former one corresponds to (6). Thus, substituting (10) into the third term of (6) yields

$$\sum_{l=1}^{3} r_l{}^\wedge\tfrac{\partial\mathcal{L}}{\partial r_l} = \tfrac{1}{2}\sum_{i=1}^{6+n}\sum_{j=1}^{6+n}\sum_{l=1}^{3} r_l{}^\wedge\tfrac{\partial m_{ij}}{\partial r_l}\dot{q}_i\dot{q}_j - \sum_{l=1}^{3} r_l{}^\wedge\tfrac{\partial\mathcal{U}}{\partial r_l}. \tag{12}$$

Note that (11) is included where k is replaced with i in the first term of the right hand side of (12). For the case of $k \neq 4,5,6$, this accords with (5) and (7) which are identical to the standard Euler-Lagrange equation. This then implies we can calculate C that guarantees the skew-symmetricity of $\dot{M}-2C$ by dividing into the sub-matrices $C = C_1 + C_2$:

$$C_{1_{kj}} = \sum_{i=1}^{6+n}\frac{1}{2}\left(\frac{\partial m_{kj}}{\partial q_i} + \frac{\partial m_{ki}}{\partial q_j} - \frac{\partial m_{ij}}{\partial q_k}\right)\dot{q}_i$$
$$C_2 = \begin{bmatrix} 0_{3\times3} & 0_{3\times3} & 0_{3\times n}\\ 0_{3\times3} & -\left(\frac{\partial\mathcal{L}}{\partial\omega}\right)^\wedge & 0_{3\times n}\\ 0_{3\times3} & 0_{3\times3} & 0_{3\times n}\end{bmatrix} \tag{13}$$

In the derivation, the vector cross product identity is used. One may notice that $\dot{M}-C_1$ is skew-symmetric since C_1 exhibits the structure similar to the Christoffel symbol. Hence, the skew-symmetricity of $\dot{M}-2C$ is guaranteed because $\dot{M}-2C_1$ is skew-symmetric and C_2 itself is a skew-symmetric matrix.

Lastly, G in (9) can be simply calculated from (5)-(7)

$$G = \begin{bmatrix} m_c g e_3\\ \sum_{i=1}^{n} m_i g\left(p_i^B\right)^\wedge R^\top e_3\\ \sum_{i=1}^{n} m_i g J_{i,t}^\top R^\top e_3\end{bmatrix} \tag{14}$$

where $m_c := m_b + \sum_{i=1}^{n} m_i$.

D. Passive Decomposition

To facilitate the controller design, passive decomposition is applied to decouple the translational dynamics from (9). Similar to [13], let us first define a new coordinate $\nu \in \mathbb{R}^{6+n}$ such that $\dot{q} = \tilde{S}\nu$ where

$$\tilde{S} = \begin{bmatrix} I_{3\times3} & -M_t^{-1}M_{tr}\\ 0_{3+n\times3} & I_{3+n\times3+n}\end{bmatrix},\quad M = \begin{bmatrix} M_t & M_{tr}\\ M_{tr}^\top & M_r\end{bmatrix}.$$

Denoting the center of mass position of the entire system as p_c and further defining $\dot{r} := [\omega^\top\ \dot{\theta}^\top]^\top \in \mathbb{R}^{3+n}$, (1)-(4) and (8) ensures $\dot{p}_c = \dot{p} - S\dot{r}$ where $S = -M_t^{-1}M_{tr}$. This implies that the new coordinate is $\nu = [\dot{p}_c^\top\ \dot{r}^\top]^\top$. Hence, substituting $\dot{q}$ with $\tilde{S}\nu$ and pre-multiplying $\tilde{S}^\top$ to (9), the equation of motion is turned into the following form

$$\tilde{M}\dot{\nu} + \tilde{C}\nu + \tilde{G} = \tilde{S}\tau \tag{15}$$

where $\tilde{M} = \tilde{S}^\top M\tilde{S}$, $\tilde{C} = \tilde{S}^\top(M\dot{\tilde{S}} + C\tilde{S})$, and $\tilde{G} = \tilde{S}^\top G$. The skew-symmetricity of $\dot{\tilde{M}} - 2\tilde{C}$ is also assured by simple calculation. Meanwhile, from (13), the top three rows of C can be rewritten as $\dot{M}_{tr}\dot{r}$ because M does not depend on p and $M_t = m_c I_{3\times3}$. Thus, the extracted translational dynamics from (9) is $M_t\ddot{p} + M_{tr}\ddot{r} + \dot{M}_{tr}\dot{r} + m_c g e_3 = TRe_3$. By substituting $\dot{p}$ with $\dot{p}_c + S\dot{r}$, this can be rewritten as

$$m_c\ddot{p}_c + m_c g e_3 = TRe_3 \tag{16}$$

Since the gravity effect term in (15) $S^\top G_p + G_r$ is cancelled out due to (14) with elements of M_t and M_{tr}, the remaining attitude and joint angle dynamics can be taken as follows:

$$\dot{R} = R\omega^\wedge$$
$$M_E\ddot{r} + C_E\dot{r} - C_{LE}^\top\dot{p}_c = \begin{bmatrix} u_b\\ u_\theta\end{bmatrix} + S^\top TRe_3 \tag{17}$$

where definitions of M_E, C_E, and C_{LE} are same with [13]. The skew-symmetricity of $\dot{M}_E - 2C_E$ also holds, and M_E is the symmetric and positive definite inertia matrix [14]. The difference between (17) and the decomposed dynamics from [13] is that C_{LE} is not zero matrix any more. This is because when C is calculated via (13), $\dot{p}$ is included. This term can be vanished if $\mathsf{SO}(3)$ is parametrized by ZYX Euler angles ($\mathbb{R}^3$) but singularity arises.

III. CONTROLLER DESIGN

Due to underactuatedness of the platform, it is impossible to follow arbitrarily assigned desired position and attitude of the multirotor base simultaneously. This study presents a control law to follow a given trajectory of desired position, body x-axis and joint angles.

A. Tracking Controller Design

Suppose that a smooth trajectory $p_{c_d}(t), B_{1_d}(t)$, and $\theta_d(t)$ is given where $p_{c_d}(t)$, $B_{1_d}(t)$, and $\theta_d(t)$ are the desired center of mass position of the aerial manipulator, the desired body x-axis of the multirotor base which corresponds to the yaw angle, and the desired joint angles, respectively. Then, error variables for the position and joint angle can be selected as $e_p = p_c - p_{c_d}$ and $e_\theta = \theta - \theta_d$. Attitude error function and error variables are chosen as [6]:

$$\Psi(R, R_d) = \tfrac{1}{2}\mathrm{tr}[I_{3\times3} - R_d^\top R]$$
$$e_R = \tfrac{1}{2}(R_d^\top R - R^\top R_d)^\vee, \; e_\omega = \omega - R^\top R_d\omega_d$$

where R_d is the desired attitude. The desired attitude is selected as $R_d = [b_{1_d} \;\; b_{3_d} \times b_{1_d} \;\; b_{3_d}]$. Here, the given B_{1_d} is slightly modified to b_{1_d} by Gram-Schmidt orthonormalization with repect to b_{3_d} calculated from the following equation

$$b_{3_d} = \frac{-K_{p_0}e_p - K_{p_1}\dot{e}_p + m_c g e_3 + m_c\ddot{p}_{c_d}}{\|-K_{p_0}e_p - K_{p_1}\dot{e}_p + m_c g e_3 + m_c\ddot{p}_{c_d}\|} \tag{18}$$

where K_{p_0} and K_{p_1} are positive diagonal gain matrices.

Assumption 1: The denominator of (18) and $\|B_{1_d} \times b_{3_d}\|$ are not zero for all $t \geq 0$.

Assumption 2: $\ddot{p}_{c_d}(t)$ is uniformly bounded, and thus there exists a positive constant B_T such that $\|m_c g e_3 + m_c\ddot{p}_{c_d}\| \leq B_T$.

Assumption 3: There exist positive constants M_l and M_u such that $0 < M_l \leq \|M_E\| \leq M_u < \infty$. This assumption has been widely adopted for many studies which deal with serially connected multi-body system. Once this assumption holds, there also exist positive constants $M_{i,l}$ and $M_{i,u}$ such that $0 < M_{i,l} \leq \|M_E^{-1}\| \leq M_{i,u} < \infty$.

To follow the trajectory p_{c_d}, b_{1_d} and θ_d, the control inputs are chosen as follows:

$$T = (-K_{p_0}e_p - K_{p_1}\dot{e}_p + m_c g e_3 + m_c\ddot{p}_{c_d})^\top R e_3 \tag{19}$$

$$u_{b,\theta} = M_E \begin{bmatrix} -\omega^\wedge R^\top R_d\omega_d + R^\top R_d\dot{\omega}_d \\ \ddot{\theta}_d \end{bmatrix} + C_E \begin{bmatrix} R^\top R_d\omega_d \\ \dot{\theta}_d \end{bmatrix}$$
$$- S^\top T R e_3 - C_{LE}^\top \dot{p}_c + \begin{bmatrix} -K_R e_R - K_\omega e_\omega \\ -K_{\theta_0}e_\theta - K_{\theta_1}\dot{e}_\theta \end{bmatrix} \tag{20}$$

where $u_{b,\theta} = [u_b^\top \;\; u_\theta^\top]^\top$. $K_R, K_\omega, K_{\theta_0}$ and K_{θ_1} are all positive diagonal gain matrices. Therefore, the closed-loop error dynamics are

$$m_c\ddot{e}_p = -K_{p_0}e_p - K_{p_1}\dot{e}_p + \|\Delta\|\{(b_{3_d}^\top b_3)b_3 - b_{3_d}\}$$
$$M_E\ddot{e}_r = -C_E\dot{e}_r + \begin{bmatrix} -K_R e_R - K_\omega e_\omega \\ -K_{\theta_0}e_\theta - K_{\theta_1}\dot{e}_\theta \end{bmatrix}$$

where $\dot{e}_r := [e_\omega^\top \;\; \dot{e}_\theta^\top]^\top$, $\Delta := -K_{p_0}e_p - K_{p_1}\dot{e}_p + m_c g e_3 + m_c\ddot{p}_{c_d}$ and $b_3 = Re_3$, respectively.

B. Stability Analysis

The stability analysis is devided into three steps: 1) almost global exponential stability of the attitude and joint angle error dynamics, 2) local exponential stability of the complete system, and 3) almost global exponential attractiveness of complete system. All of the geometric properties used to prove propositions are summarized in [15].

Proposition 1: (Almost global exponential stability of attitude and joint angle error dynamics) The zero equilibrium of $\dot{e}_r$, e_R, and e_θ is exponentially stable. Moreover, the error function $\Psi(R(t), R_d(t))$ decreases exponentially with the following region of attraction:

$$\Psi(R(0), R_d(0)) < 2$$

$$\lambda_M(M_E(0))\|\dot{e}_r(0)\|^2 + \lambda_M(K_{\theta_0})\|e_\theta(0)\|^2 < 2\lambda_m(K_R)(2 - \Psi(R(0), R_d(0))) \tag{21}$$

Proof: Consider a positive definite function V_1' as

$$V_1' = \tfrac{1}{2}\dot{e}_r^\top M_E\dot{e}_r + \lambda_m(K_R)\Psi(R, R_d) + \tfrac{1}{2}e_\theta^\top K_{\theta_0}e_\theta. \tag{22}$$

Since $\frac{d}{dt}R_d^\top R = R_d^\top R e_\omega^\wedge$ and $\mathrm{tr}(R_d^\top R e_\omega^\wedge) = \mathrm{tr}(e_\omega^\wedge e_R^\wedge) = -2e_R^\top e_\omega$, the time derivative of (22) is bounded by

$$\dot{V}_1' \leq -e_\omega^\top K_\omega e_\omega - \dot{e}_\theta^\top K_{\theta_1}\dot{e}_\theta \leq 0.$$

In the derivation, the skew-symmetricity of $\dot{M}_E - 2C_E$ is used. This implies that $V_1'(t) \leq V_1'(0)$ holds for any $t \geq 0$. With (21), the following inequality is satisfied.

$$\lambda_m(K_R)\Psi(R(t), R_d(t)) \leq V_1'(t) \leq V_1'(0) < 2\lambda_m(K_R)$$

Thus, there exists a positive constant ψ_1 such that $\Psi(R, R_d) \leq \psi_1 < 2$ for any $t \geq 0$. Furthermore, the following inequality holds [15].

$$\tfrac{1}{2}\|e_R\|^2 \leq \Psi(R, R_d) \leq \tfrac{1}{2-\psi_1}\|e_R\|^2 \tag{23}$$

Now, for a positive constant α_1, let a lyapunov candidate function for the attitude and joint angle error dynamics V_1 be

$$V_1 = V_1' + \alpha_1[e_R^\top \; e_\theta^\top]\,\dot{e}_r. \tag{24}$$

From (23) and *Assumption* 3, V_1 is bounded by $z_1^\top P_l z_1 \leq V_1 \leq z_1^\top P_u z_1$ where $z_1 = [\|e_R\|, \; \|e_\omega\|, \; \|e_\theta\|, \; \|\dot{e}_\theta\|]^\top$ and

$$P_l = \frac{1}{2}\begin{bmatrix} \lambda_m(K_R) & -\alpha_1 & 0 & -\alpha_1 \\ -\alpha_1 & M_l & -\alpha_1 & 0 \\ 0 & -\alpha_1 & \lambda_m(K_\theta) & -\alpha_1 \\ -\alpha_1 & 0 & -\alpha_1 & M_l \end{bmatrix}$$
$$P_u = \frac{1}{2}\begin{bmatrix} \frac{2\lambda_m(K_R)}{2-\psi_1} & \alpha_1 & 0 & \alpha_1 \\ \alpha_1 & M_u & \alpha_1 & 0 \\ 0 & \alpha_1 & \lambda_M(K_\theta) & \alpha_1 \\ \alpha_1 & 0 & \alpha_1 & M_u \end{bmatrix} \tag{25}$$

The time derivative of (24) is upper bounded by

$$\dot{V}_1 \leq -e_\omega^\top K_w e_\omega - \dot{e}_\theta^\top K_{\theta_1}\dot{e}_\theta + \alpha_1\dot{e}_R^\top e_\omega + \alpha_1\|\dot{e}_\theta\|^2 +$$
$$\alpha_1[e_R^\top \; e_\theta^\top]M_E^{-1}\left(-\begin{bmatrix} K_R e_R \\ K_{\theta_0}e_\theta \end{bmatrix} - N\begin{bmatrix} e_\omega \\ \dot{e}_\theta \end{bmatrix}\right) \tag{26}$$

where $N = C_E + \mathtt{blkdiag}\{K_\omega I_{3\times3}, \; K_{\theta_1}I_{3\times3}\}$. For the third term above, as per [6], $\|\dot{e}_R\| \leq \|e_\omega\|$ holds. Thus, (26) is turned into the following inequality.

$$\dot{V}_1 \leq -z_1^\top P_d z_1 \tag{27}$$

$$P_d = \begin{bmatrix} \alpha_1 p_{11} & -\alpha_1 p_{12} & 0 & -\alpha_1 p_{12} \\ -\alpha_1 p_{12} & p_{13} - \alpha_1 & -\alpha_1 p_{12} & 0 \\ 0 & -\alpha_1 p_{12} & \alpha_1 p_{11} & -\alpha_1 p_{12} \\ -\alpha_1 p_{12} & 0 & -\alpha_1 p_{12} & p_{14} - \alpha_1 \end{bmatrix}$$

where $p_{11} = \min(\lambda_m(K_R), \lambda_m(K_{\theta_0}))/M_u$, $p_{12} = C_u M_{i,u} + \max(\lambda_M(K_\omega), \lambda_M(K_{\theta_1}))M_{i,u}$, $p_{13} = \lambda_m(K_\omega)$ and $p_{14} = \lambda_m(K_{\theta_1})$ are all positive constants. Here, C_u is a positive constant such that $\|C_E\| \leq C_u$.

To derive further, positive definiteness of P_l, P_u and P_d is required. Through simple computation of checking positive definiteness of the matrices, a positive constant α_1 always exists for any arbitrarily large C_u. Thus, with the positive-definite matrices, below inequality holds.

$$\lambda_m(P_l)\|z_1\|^2 \leq V_1 \leq \lambda_M(P_u)\|z_1\|^2$$
$$\dot{V}_1 \leq -\lambda_m(P_d)\|z_1\|^2 \leq -\frac{\lambda_m(P_d)}{\lambda_M(P_u)}V_1$$

This leads $V_1(t) \leq V_1(0)e^{-\beta_1 t}$ where $\beta_1 = \frac{\lambda_m(P_d)}{\lambda_M(P_u)}$. Therefore, we can conclude that the zero equilibrium of $\dot{e}_r$, e_R, and e_θ is exponentially stable. Furthermore, from (23) and the above bounds of V_1, one can induce the exponential decrease of $\Psi(R, R_d)$ as the following:

$$\begin{aligned}\lambda_m(P_l)(2-\psi_1)\Psi(R, R_d) &\leq \lambda_m(P_l)\|e_R\|^2 \\ &\leq V_1(t) \leq V_1(0)e^{-\beta_1 t}\end{aligned}$$

This completes the proof. ■

Remark 1: This proposition guarantees the exponential stability unless R_d is exactly rotated 180° with respect to R for some axis. Also the larger K_R is chosen, the larger the region of attraction (21) becomes.

Proposition 2: (Local exponential stability of the complete system) The zero equilibrium of e_p, $\dot{e_p}$, $\dot{e}_r$, e_R, and e_θ is exponentially stable. The region of attraction is as follows:

$$\Psi(R(0), R_d(0)) < 1 \tag{28}$$

$$\begin{aligned}\lambda_M(M_E(0))\|\dot{e}_r(0)\|^2 + \lambda_M(K_{\theta_0})\|e_\theta(0)\|^2 < \\ 2\lambda_m(K_R)(1-\Psi(R(0), R_d(0)))\end{aligned} \tag{29}$$

Proof: (28) and (29) satisfy the conditions for *Proposition* 1. This implies that we can directly utilize the result and analysis of it. Thus, there exists a positive constant ψ_2 such that $\Psi(R, R_d) \leq \psi_2 < 1$ for any $t \geq 0$. For the quantity $\|(b_{3_d}^\top b_3)b_3 - b_{3_d}\|$, the following inequality holds [15].

$$\|(b_{3_d}^\top b_3)b_3 - b_{3_d}\| \leq \|e_R\| \leq \zeta := \sqrt{\psi_2(2-\psi_2)} < 1 \tag{30}$$

For a negative constant α_2, consider a function V_2' as

$$V_2' = \tfrac{1}{2}\dot{e}_p^\top m_c \dot{e}_p + \tfrac{1}{2}e_p^\top K_{p_0} e_p + \alpha_2 e_p^\top \dot{e}_p.$$

Then, the time derivative of V_2' is upper bounded by

$$\begin{aligned}\dot{V}_2' \leq& -(\lambda_m(K_{p_1})-\alpha_2)\|\dot{e}_p\|^2 - \alpha_2 m_c^{-1}\lambda_m(K_{p_0})\|e_p\|^2 \\ &+ \alpha_2 m_c^{-1}\lambda_M(K_{p_1})\|e_p\|\|\dot{e}_p\| + (\|\dot{e}_p\| + \alpha_2 m_c^{-1}\|e_p\|)\Xi\end{aligned}$$

where $\Xi = \|\Delta\|\{(b_{3_d}^\top b_3)b_3 - b_{3_d}\}$. Thanks to $Assumption$ 2 and (30), the following inequality is induced from the above $\dot{V}_2'$:

$$\begin{aligned}\dot{V}_2' \leq& \alpha_2 s_{21}\|e_p\|^2 + (s_{24}+\alpha_2)\|\dot{e}_p\|^2 + (\alpha_2 s_{22} + s_{23})\|e_p\| \\ &\times \|\dot{e}_p\| + B_T\|\dot{e}_p\|\|e_R\| + \alpha_2 m_c^{-1}B_T\|e_p\|\|e_R\|\end{aligned} \tag{31}$$

where $s_{21} = m_c^{-1}(\lambda_M(K_{p_0})\zeta - \lambda_m(K_{p_0}))$, $s_{22} = m_c^{-1}\lambda_M(K_{p_1})(1+\zeta)$, $s_{23} = \lambda_M(K_{p_0})\zeta$ and $s_{24} = \lambda_M(K_{p_1})\zeta - \lambda_m(K_{p_1})$, respectively. These are all positive with $\zeta > \max(\frac{\lambda_m(K_{p_0})}{\lambda_M(K_{p_0})}, \frac{\lambda_m(K_{p_1})}{\lambda_M(K_{p_1})})$. If all elements of each gain matrix are the same, this proposition could be proved in the same manner with [15].

Now, let a Lyapunov candidate function for the complete dynamics be $V_2 = V_1 + V_2'$. From (27) and (31), the time derivative of V_2 can be represented as follows:

$$\dot{V}_2 \leq -z_1^\top P_d z_1 + z_2^\top S_1 z_1 - z_2^\top S_2 z_2 = -z^\top S z$$

$$z = \begin{bmatrix} z_1 \\ z_2 \end{bmatrix}, \quad z_2 = \begin{bmatrix} \|e_p\| \\ \|\dot{e}_p\| \end{bmatrix}, \quad S = \begin{bmatrix} P_d & -\frac{1}{2}S_1 \\ -\frac{1}{2}S_1^\top & S_2 \end{bmatrix},$$

$$S_2 = -\begin{bmatrix} \alpha_2 s_{21} & \alpha_2 s_{22} + s_{23} \\ \alpha_2 s_{22} + s_{23} & s_{24} + \alpha_2 \end{bmatrix}, S_1^\top = \begin{bmatrix} \alpha_2 s_{11} & 0_{1\times 3} \\ s_{12} & 0_{1\times 3} \end{bmatrix}$$

where $s_{11} = m_c^{-1}B_T$, and $s_{12} = B_T$, respectively. In the above inequality, P_d is already positive-definite. Then, by Schur's complement theorem, S is positive-definite if and only if $S_2 - \frac{1}{4}S_1^\top P_d^{-1} S_1$ is positive-definite. Also, V_2 can be rewritten as the following bounded inequality.

$$z_1^\top P_l z_1 + z_2^\top Q_l z_2 \leq V_2 \leq z_1^\top P_u' z_1 + z_2^\top Q_u z_2 \tag{32}$$

$$Q_l = \frac{1}{2}\begin{bmatrix} \lambda_M(K_{p_0}) & -\alpha_2 \\ -\alpha_2 & m_c \end{bmatrix}, \quad Q_u = \frac{1}{2}\begin{bmatrix} \lambda_M(K_{p_0}) & \alpha_2 \\ \alpha_2 & m_c \end{bmatrix}$$

where P_u' is identical to (25) except for the first diagonal element replaced with $\frac{2\lambda_m(K_R)}{2-\psi_2}$.

Hence, similar to the *Proposition* 1, there exists α_1^* such that, for each $0 < \alpha_1 < \alpha_1^*$, P_d, P_l, and P_u' become positive definite. Concurrently, there exists α_2^* such that, for each $\alpha_2^* < \alpha_2 < 0$, positive-definiteness of Q_l, Q_u and S is guaranteed. Here, S is positive definite if the range of α_2 such that $\lambda_m(P_d) > \frac{\|S_1\|^2}{4\lambda_m(S_2)}$ is found. Now, defining positive definite matrices $R_u := \mathtt{blkdiag}\{Q_u, P_u'\}$ and $R_l := \mathtt{blkdiag}\{Q_l, P_l'\}$, (32) can be reformulated into $z^\top R_l z \leq V_2 \leq z^\top R_u z$, and the exponential stability of the complete dynamics is shown as $V_2(t) \leq V_2(0)e^{-\beta_2 t}$, $\beta_2 = \frac{\lambda_m(S)}{\lambda_M(R_u)}$. ■

Remark 2: Proposition 2 only considers the case when initial attitude error is less than 90°. If (28) is not satisfied, the direction of body z-axis where the net thrust is generated faces the opposite direction to e_p and thus the monotonically exponential decrease of translational error may not be guaranteed. However, even though the initial condition does not meet (28), it will be eventually satisfied in a finite time $t^* > 0$ by *Proposition* 1 and all error starts to decrease exponentially if $\|e_p\|$ and $\|\dot{e}_p\|$ are bounded during attitude recovery. Hence, the almost global exponential attractiveness for the complete system can be simply proved by showing the boundedness of $\|e_p\|$ and $\|\dot{e}_p\|$ for any finite time t^*.

Proposition 3: (Almost global exponential attractiveness of the complete system) Suppose that the initial condition satisfies

$$1 \leq \Psi(R(0), R_d(0)) < 2$$

$$\begin{aligned}\lambda_M(M_E(0))\|\dot{e}_r(0)\|^2 + \lambda_M(K_{\theta_0})\|e_\theta(0)\|^2 < \\ 2\lambda_m(K_R)(2-\Psi(R(0), R_d(0)))\end{aligned}$$

Then, there exist t^* such that the zero equilibrium of e_p, $\dot{e}_p$, e_R, e_θ and $\dot{e}_r$ is exponentially stable for $t > t^* > 0$. Also, $\|e_p\|$ and $\|\dot{e}_p\|$ are bounded in the time interval $0 \leq t \leq t^*$.

Proof: Since the proof is similar to [15] the procedure is omitted due to page limit. ■

Remark 3: This proposition states that, even for huge initial attitude error, the error is always finite during the transient attitude recovery phase. Also, the error variables for complete system enter the region of attraction for *Proposition* 2 and eventually exponentially decrease.

IV. EXPERIMENTAL RESULT

A. Experimental setup

The aerial manipulator is built with a single 2-DOF manipulator attatched hexarotor. TAROT S550 hexacopter frame is used as the multirotor base. Since servomotors have to be commanded to generate joint torques from the controller, we adopted two ROBOTIS Dynamixel XM-430 series servomotors which enable the current control mode. Because the net thrust calculated from (19) can be negative, we used six pairs of APC 9×4.5R propellers and KDE2315XF-965 BLDC motors and two XRotor Micro 40A 6S 4in1 ESCs for bidirectional thrust generating system. For an onboard computer to calculate control inputs, Intel NUC running Robot Operating System (ROS) in Ubuntu 18.04 is mounted. Calculated thrust and body torques are tossed to Pixhawk 4 which runs appropriately customized PX4 firmware for bidirectional setup to convert control inputs to thrusts for each rotor. Here, thrust and body torques are normalized with respect to the maximum thrust and torque values respectively. Computed joint torques are commanded to servomotors after converted to corresponding currents via the torque and current relationship. Optitrack motion capture system is used for multirotor base localization.

B. Aerial flipping

To validate the proposed method, two successive aerial flipping is performed while the desired joint angles are stationary. The aerial flipping command can be given simply changing the sign of desired body z-axis (18). In experiment, I gain is slightly added to compensate the real-time battery consumption and error in the model parameter identification.

Figs. 3 and 4 show the result of two successive aerial flipping. Shaded areas in both figures indicate the inverted flight phase. This experiment validates the almost global attractiveness of the proposed controller. From fig. 3, although the initial attitude error is almost 180° for each flip, the exponential decrease of Ψ is observed. This coincides with *Proposition* 1. Meanwhile, the initial increase of $\|e_p\|$ but boundedness can be seen. As anticipated, this is because the initial condition is out of the region of attraction of *Proposition* 2. However, the translational error eventually decreases exponentially by *Proposition* 3. Fig. 4 presents control input history. When the flight mode is changed from normal flight to inverted flight and vice versa, the sign of thrust automatically changes in order to hover in free space.

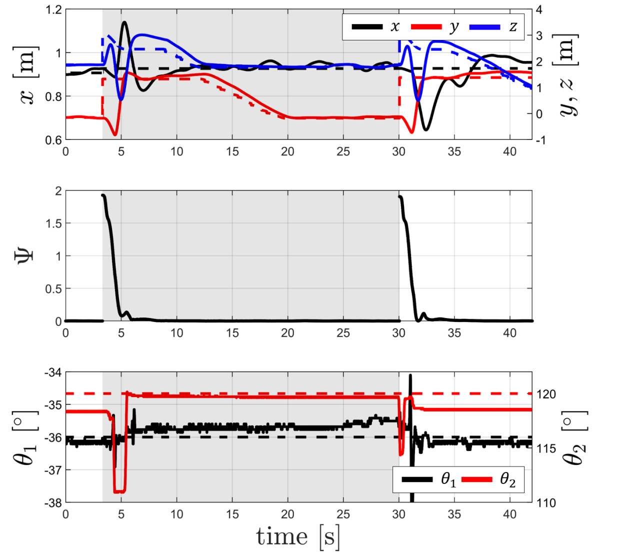

Fig. 3. Time history of state variables. From the top, each plot describes the center of mass position, attitude and joint angles, respectively. Solid line and dashed line indicate actual and desired value, respectively.

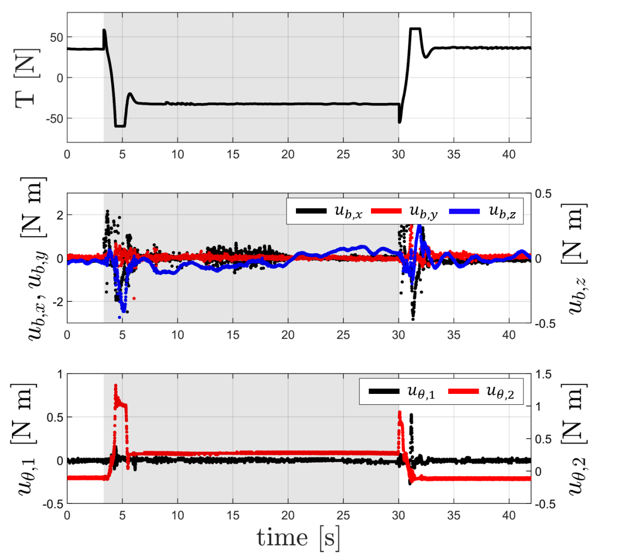

Fig. 4. Time history of control inputs

V. CONCLUSIONS

This article presents the reformulated dynamics of a conventional multirotor equipped with n-DOF robotic manipulator using modified Lagrangian dynamics. Direct derivation of the attitude dynamics on $\mathsf{SO}(3)$ is enabled without using local coordinate such as euler angle representation. Since the newly derived Lagrangian dynamics differs from standard one, we propose a method to compute the Coriolis matrix which guarantees the skew-symmetric property with the inertia matrix. Furthermore, passive decomposition into translational dynamics and remaining attitude and joint angle dynamics is applied to facilitate the controller design and stability analysis. With the decoupled dynamics, a geometric tracking controller is designed which guarantees almost global region of attraction. We successfully demonstrated the proposed method through real experiments of consecutive aerial flipping. Thanks to the general description of this paper, designing a model-free robust controller based on the proposed globally defined dynamics is considered as future work.

REFERENCES

[1] G. Garimella and M. Kobilarov, “Towards model-predictive control for aerial pick-and-place,” in *2015 IEEE international conference on robotics and automation (ICRA)*. IEEE, 2015, pp. 4692–4697.

[2] A. Jimenez-Cano, J. Braga, G. Heredia, and A. Ollero, “Aerial manipulator for structure inspection by contact from the underside,” in *2015 IEEE/RSJ international conference on intelligent robots and systems (IROS)*. IEEE, 2015, pp. 1879–1884.

[3] D. Lee, H. Seo, I. Jang, S. J. Lee, and H. J. Kim, “Aerial manipulator pushing a movable structure using a dob-based robust controller,” *IEEE Robotics and Automation Letters*, vol. 6, no. 2, pp. 723–730, 2020.

[4] J. Byun, D. Lee, H. Seo, I. Jang, J. Choi, and H. J. Kim, “Stability and robustness analysis of plug-pulling using an aerial manipulator,” in *2021 IEEE/RSJ International Conference on Intelligent Robots and Systems (IROS)*. IEEE, 2021, pp. 4199–4206.

[5] S. Kim, S. Choi, and H. J. Kim, “Aerial manipulation using a quadrotor with a two dof robotic arm,” in *2013 IEEE/RSJ International Conference on Intelligent Robots and Systems*. IEEE, 2013, pp. 4990–4995.

[6] T. Lee, M. Leok, and N. H. McClamroch, “Geometric tracking control of a quadrotor uav on se (3),” in *49th IEEE conference on decision and control (CDC)*. IEEE, 2010, pp. 5420–5425.

[7] ——, “Geometric tracking control of a quadrotor uav for extreme maneuverability,” *IFAC Proceedings Volumes*, vol. 44, no. 1, pp. 6337–6342, 2011.

[8] T. Fernando, J. Chandiramani, T. Lee, and H. Gutierrez, “Robust adaptive geometric tracking controls on so (3) with an application to the attitude dynamics of a quadrotor uav,” in *2011 50th IEEE conference on decision and control and European control conference*. IEEE, 2011, pp. 7380–7385.

[9] T. Lee, M. Leok, and N. H. McClamroch, “Nonlinear robust tracking control of a quadrotor uav on se (3),” *Asian journal of control*, vol. 15, no. 2, pp. 391–408, 2013.

[10] ——, “Global formulations of lagrangian and hamiltonian dynamics on manifolds,” *Springer*, vol. 13, pp. 274–280, 2017.

[11] H. Lee and H. J. Kim, “Constraint-based cooperative control of multiple aerial manipulators for handling an unknown payload,” *IEEE Transactions on Industrial Informatics*, vol. 13, no. 6, pp. 2780–2790, 2017.

[12] Y. Chen, J. Liang, Y. Wu, Z. Miao, H. Zhang, and Y. Wang, “Adaptive sliding-mode disturbance observer-based finite-time control for unmanned aerial manipulator with prescribed performance,” *IEEE Transactions on Cybernetics*, 2022.

[13] H. Yang and D. Lee, “Dynamics and control of quadrotor with robotic manipulator,” in *2014 IEEE international conference on robotics and automation (ICRA)*. IEEE, 2014, pp. 5544–5549.

[14] D. Lee, “Passive decomposition and control of nonholonomic mechanical systems,” *IEEE Transactions on Robotics*, vol. 26, no. 6, pp. 978–992, 2010.

[15] T. Lee, M. Leok, and N. H. McClamroch, “Control of complex maneuvers for a quadrotor uav using geometric methods on se(3),” 2010. [Online]. Available: https://arxiv.org/abs/1003.2005